

*Ab initio* calculations of ideal tensile strength and mechanical stability in copper

This article has been downloaded from IOPscience. Please scroll down to see the full text article.

2004 J. Phys.: Condens. Matter 16 1045

(<http://iopscience.iop.org/0953-8984/16/7/004>)

View [the table of contents for this issue](#), or go to the [journal homepage](#) for more

Download details:

IP Address: 129.252.86.83

The article was downloaded on 27/05/2010 at 12:43

Please note that [terms and conditions apply](#).

## ***Ab initio* calculations of ideal tensile strength and mechanical stability in copper**

M Černý<sup>1</sup>, M Šob<sup>2</sup>, J Pokluda<sup>1</sup> and P Šandera<sup>1</sup>

<sup>1</sup> Institute of Engineering Physics, Faculty of Mechanical Engineering, Brno University of Technology, Technická 2, CZ-616 69 Brno, Czech Republic

<sup>2</sup> Institute of Physics of Materials, Academy of Sciences of the Czech Republic, Žitkova 22, CZ-616 62 Brno, Czech Republic

E-mail: mcerny@ipm.cz

Received 13 November 2003

Published 6 February 2004

Online at [stacks.iop.org/JPhysCM/16/1045](http://stacks.iop.org/JPhysCM/16/1045) (DOI: 10.1088/0953-8984/16/7/004)

### **Abstract**

A simulation of a tensile test of copper crystal along the [001] direction is performed using the Vienna *ab initio* simulation package (VASP). Stability conditions for a uniaxially loaded system are presented and analysed and the ideal (theoretical) tensile strength for the loading along the [001] direction is determined to be 9.4 GPa in tension and 3.5 GPa in compression. A comparison with experimental values is performed.

### **1. Introduction**

In most engineering applications, the strength of materials is controlled by nucleation and motion of dislocations and microcracks. If such defects were not present, the material would only fail if the limit of elastic stability were reached. The stress at which this is achieved is an upper limit of stresses attainable prior to failure and is called the ideal (theoretical) strength. Until recently, loads of this magnitude were approached in studies of the mechanical behaviour of whiskers of very pure metals and semiconductors. However, knowledge of the ratio of the tensile and shear ideal strengths allows the assessment of both the ductile/brittle response and the crack stability in solids [1]. The ideal strength appears to control both the onset of fracture and the dislocation nucleation in defect-free thin films and, in particular, in nanostructured materials that are currently being developed. This has been confirmed most eloquently by nanoindentation experiments (see e.g. [2] and references therein) which suggest that the onset of yielding on the nanoscale is controlled by homogeneous nucleation of dislocations in the small volume under the nanoindenter where stresses approach the ideal strength.

To predict the ideal strength, we have to check the elastic stability criteria under increasing external load. The criterion which is violated first sets the ideal strength.

Theoretically, the ideal strength was studied in the past using semiempirical approaches when describing interatomic interactions (see e.g. [3]). However, within such schemes

parameters are fitted predominantly to equilibrium properties of the material studied and their transferability to the state when the material is loaded close to its theoretical strength is not guaranteed. In contrast, *ab initio* electronic structure calculations can be performed reliably for variously strained structures and are thus capable of determining the ideal strength of materials without resort to doubtful extrapolations. Indeed, recently, determination of ideal strength became possible using *ab initio* electronic structure methods based on the density functional theory.

In this paper we study the ideal tensile strength of copper in the [001] direction. This is a continuation of the previous *ab initio* investigation [4], where, similarly as in several other *ab initio* studies, only one criterion of the mechanical stability, i.e. the positive value of the Young modulus, was used, and the calculated ideal tensile strength for the [001] loading, 33 GPa, was more than an order of magnitude higher than the experimental value of about 1.5 GPa (see [5]). Let us note that studies investigating the ideal strength of copper using the Morse potential [3] and the embedded-atom method [6] found an elastic instability prior to reaching the zero value of the Young modulus (i.e., the inflection point in the energy versus strain curve) at the stresses of 6.97 and 9.82 GPa, respectively, still considerably higher than the experimental result. Here we simulate a tensile test of copper from first principles for uniaxial loading in the [001] direction, analysing all stability criteria, and determine the corresponding ideal tensile strength.

## 2. Details of calculations

To simulate a tensile test, we first calculate the total energy of the material in the ground state. In the case of copper, the ground state exhibits the face-centred cubic (fcc) structure. Then, in the second step, we apply some elongation of the crystal along the loading axis by a fixed amount  $\varepsilon$  that is equivalent to the application of a certain tensile stress  $\sigma$ . For each  $\varepsilon$ , we minimize the total energy, relaxing the stresses  $\sigma_{\perp 1} = \sigma_{\perp 2}$  in the directions perpendicular to the loading axis, i.e. relaxing the perpendicular dimensions of the crystal. Thus, we simulate a strain-controlled uniaxial loading of the crystal. The stress  $\sigma$  is given by

$$\sigma = \frac{n}{a^2} \frac{dE_{\text{tot}}}{dc} = \frac{n}{a^2 a_0} \frac{dE_{\text{tot}}}{d\varepsilon}, \quad (1)$$

where  $n$  is number of atoms in the elementary cubic or tetragonal cell (here  $n = 4$ ),  $E_{\text{tot}}$  is the total energy of a crystal per atom,  $c$  is the lattice parameter in the loading direction (see figure 1), and  $a$  is the lattice parameter in the directions perpendicular to the loading axis. Furthermore,  $a_0$  is the equilibrium lattice parameter (in the ground fcc state) and  $\varepsilon$  is the linear extension defined by the relation  $\varepsilon = c/a_0 - 1$ .

In the case of the uniaxial loading along the [001] direction, we investigate, in fact, the behaviour of the total energy along the Bain transformation path connecting the body-centred cubic (bcc) and fcc structures. If we ascribe  $c/a = 1$  to the fcc structure, then the bcc structure is obtained for  $c/a = \sqrt{1/2}$ . All other structures along this path may be considered either as face-centred tetragonal (fct) or as body-centred tetragonal (bct) [7, 8]. The Young modulus for the [001] direction is obtained according to

$$E_{[001]} = \frac{n}{a^2 a_0} \frac{d^2 E_{\text{tot}}}{d\varepsilon^2}. \quad (2)$$

Stability conditions expressed in terms of second-order elastic constants were derived e.g. in [9, 10] for a general system under arbitrary loading. Under uniaxial loading of a cubic solid along the [001] direction, the symmetry changes to tetragonal and there are six

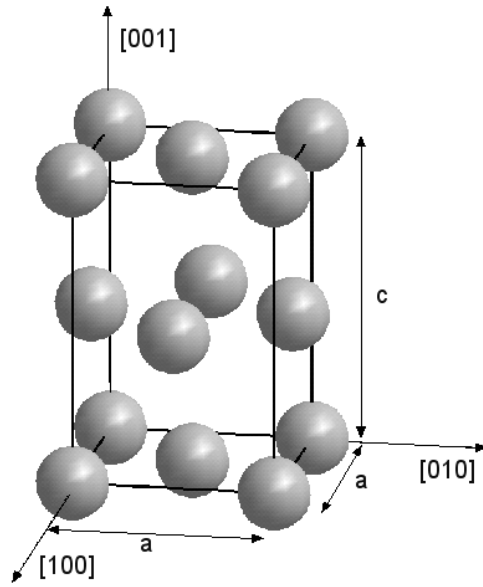


Figure 1. The elementary fct cell of uniaxially loaded copper.

independent elastic constants ( $C_{11}$ ,  $C_{12}$ ,  $C_{13}$ ,  $C_{33}$ ,  $C_{44}$ , and  $C_{66}$ ). The corresponding stability conditions are [11]

$$(C_{33} + \sigma)(C_{11} + C_{12}) - 2(C_{13} - \sigma/2)^2 > 0, \quad (3a)$$

$$C_{11} - C_{12} > 0, \quad (3b)$$

$$C_{44} + \sigma/2 > 0, \quad (3c)$$

$$C_{66} > 0. \quad (3d)$$

Here we use the elastic constants defined according to the energy expansion [12]

$$E = E(V) + V \sum_i \sigma_i \eta_i + \frac{1}{2} V \sum_i \sum_j C_{ij} \eta_i \eta_j + O(\eta^3), \quad (4)$$

where  $\eta_i$  are components of the Lagrangian strain tensor [13] in the Voigt notation.

In order to test the stability conditions, one can perform a small additional distortion (a deviation from the main tetragonal path) and check the energy change. Using a set of primitive translational vectors (i.e.  $[0, a/2, c/2]$ ,  $[a/2, 0, c/2]$ , and  $[a/2, a/2, 0]$  in our case), the distortion can be described by means of an appropriate Jacobian matrix  $\mathbf{J}$  as

$$\mathbf{r} = \mathbf{J} \cdot \mathbf{r}_T,$$

where  $\mathbf{r}_T$  is the vector corresponding to the current state along the tetragonal path and vector  $\mathbf{r}$  describes the distorted state.

The stability condition (3a) corresponds to the requirement that  $E_{[001]}$  is positive. It is related to the inflection point in the  $E_{\text{tot}}(c)$  dependence and was tested in all above-mentioned previous calculations. The right-hand side of this condition differs from the Young modulus by a multiplicative factor and the two quantities acquire the zero value simultaneously.

The stability condition (3b) is equivalent to the criterion  $C_{22} - C_{23} > 0$  presented in [3] for [100] tensile loading. Its violation corresponds to a shear instability (vanishing of the tetragonal shear modulus) when we can expect the bifurcation from the primary deformation path to a secondary one (where the lattice acquires orthorhombic symmetry). In order to test the

second stability criterion, the following Jacobian matrix (and corresponding strain matrix) [13] was used at each point of our tetragonal deformation path:

$$\mathbf{J} = \begin{pmatrix} \sqrt{1+2x} & 0 & 0 \\ 0 & \sqrt{1-2x} & 0 \\ 0 & 0 & 1 \end{pmatrix}, \quad \boldsymbol{\eta} = \begin{pmatrix} x & 0 & 0 \\ 0 & -x & 0 \\ 0 & 0 & 0 \end{pmatrix}.$$

Under such deformation, the energy of the system (per atom) changes according to the relation (see equation (4))

$$\Delta E = V (C_{11} - C_{12})x^2 + \dots,$$

where  $V = ca^2/n$  is the current volume per atom. This deformation lowers the symmetry of the crystal to the orthorhombic one and makes our calculations more time-consuming. On the other hand, the calculated  $\Delta E(x)$  curve is symmetric ( $\Delta E(x) = \Delta E(-x)$ ) and only one half of the curve has to be computed. With regard to the energy expansion, the tetragonal shear modulus  $C' = \frac{1}{2}(C_{11} - C_{12})$  can be expressed as

$$C' = \frac{1}{4V} \frac{d^2 E}{dx^2}.$$

The condition (3c) corresponds to another shear instability related to the  $C_{44}$  modulus. Using the strain

$$\boldsymbol{\eta} = \begin{pmatrix} 0 & 0 & 0 \\ 0 & 0 & x \\ 0 & x & 0 \end{pmatrix}$$

one obtains the dependence  $E(x)$  leading to

$$\Delta E = 2VC_{44}x^2 + \dots, \quad C_{44} = \frac{1}{4V} \frac{d^2 E}{dx^2}.$$

The stability condition (3d) can be tested using the strain

$$\boldsymbol{\eta} = \begin{pmatrix} 0 & x & 0 \\ x & 0 & 0 \\ 0 & 0 & 0 \end{pmatrix}.$$

The energy change of a system under such deformation and the elastic constant  $C_{66}$  can be expressed as

$$\Delta E = 2VC_{66}x^2 + \dots, \quad C_{66} = \frac{1}{4V} \frac{d^2 E}{dx^2}.$$

For the electronic structure calculations, we utilized the Vienna *ab initio* simulation package (VASP) [14] using ultrasoft pseudopotentials [15] as supplied with the code. The cut-off energy of the plane-wave basis set was 240 eV. The exchange–correlation energy was evaluated using the generalized-gradient approximation (GGA) with the parametrization of Perdew and Wang [16]. The  $20 \times 20 \times 20$   $k$ -point mesh was used in all our calculations. The solution was considered to be self-consistent when the energy difference of two subsequent iterations was smaller than 0.1 meV.

To assess the reliability of our calculations, some quantities were calculated also by means of the full-potential linearized augmented plane-wave (FLAPW) WIEN97 code described in detail in [17]. For the exchange–correlation energy, both the local density approximation (LDA) [18] and the GGA [16] were employed. The muffin-tin radius of copper atoms of 2.0 au was kept constant for all calculations, the number of  $k$ -points in the whole Brillouin zone was set to 15 000, and the product of the muffin-tin radius and the maximum reciprocal space vector,  $R_{\text{MT}}k_{\text{max}}$ , was equal to 10. The maximum  $l$  value for the waves inside the atomic spheres,  $l_{\text{max}}$ , and the largest reciprocal vector  $G$  in the charge Fourier expansion,  $G_{\text{max}}$ , were set to 12 and 15, respectively.

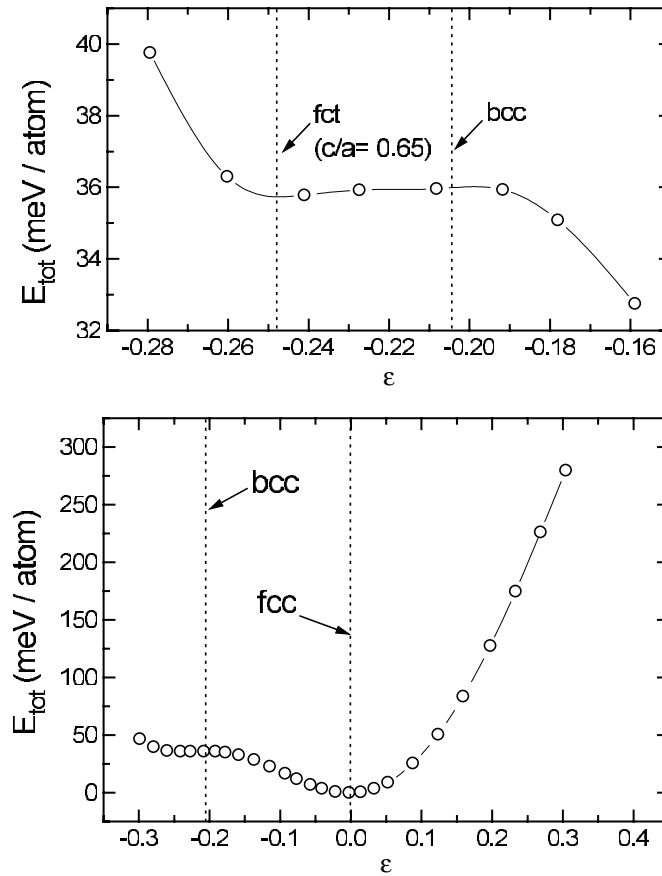


**Figure 2.** Total energy (per atom) of uniaxially deformed copper as a function of the linear extension  $\epsilon$  relative to the energy of the fcc ground state. The vertical lines represent the position of the fcc ( $\epsilon = 0$ ) and bcc ( $\epsilon = -0.205$ ) structures as well as of the fct structure corresponding to the local minimum ( $\epsilon = -0.25$ ).

### 3. Computed results and discussion

Figure 2 shows the total energy of copper as a function of  $\epsilon$  during simulated uniaxial tensile testing along the [001] direction. The curves in figure 2 were constructed by means of a cubic spline using the values of the total energy (displayed by circles) obtained by VASP GGA calculations. As expected, the main minimum of the curve corresponds to the fcc lattice (the ground-state structure). It should be emphasized that the shallow local minimum on the  $E_{\text{tot}}(\epsilon)$  curve at  $\epsilon = -0.248$  in figure 2 does not correspond to the bcc structure since the corresponding  $c/a$  ratio is about 0.65. The bcc structure ( $c/a = \sqrt{1/2}$ ) is obtained at  $\epsilon = -0.205$  corresponding rather to the local maximum between the two minima.

Values of the equilibrium lattice constant  $a_0$ , Young modulus  $E_{[001]}$  in the direction of applied load, tetragonal shear modulus  $C'$ , trigonal shear modulus  $C_{44}$ , and maximum stress  $\sigma_{E=0}$  (calculated according to equation (1)) at the inflection point of the tensile portion of the  $E_{\text{tot}}(\epsilon)$  curve are collected in table 1. For comparison, values computed using the all-electron program code WIEN97 [19] are listed together with experimental data [20–22].

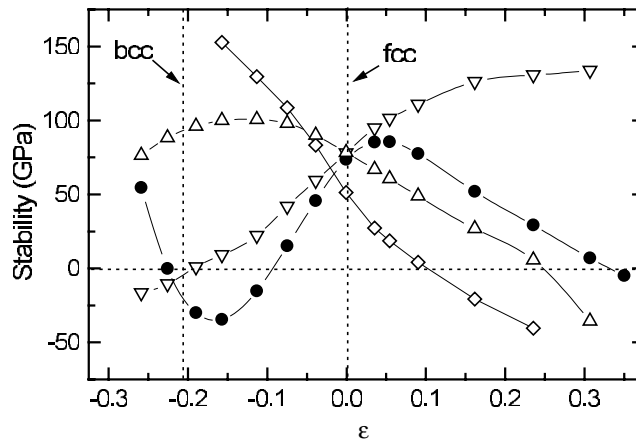


**Figure 3.** Stability conditions as functions of the linear extension  $\varepsilon$ .  $\bullet$ :  $E_{[001]}$ ,  $\diamond$ :  $C_{11} - C_{12}$ ,  $\triangle$ :  $C_{44} + \sigma/2$ ,  $\nabla$ :  $C_{66}$ .

**Table 1.** Computed values of the lattice parameter  $a_0$ , Young modulus  $E_{[001]}$ , shear moduli  $C' = \frac{1}{2}(C_{11} - C_{12})$  and  $C_{44}$  in the equilibrium state ( $\sigma = 0$ ), and stress  $\sigma_{E=0}$  at the inflection point of the tensile portion of the  $E_{\text{tot}}(\varepsilon)$  curve of the fct copper crystal.

	VASP GGA	WIEN97		Experiment
		LDA	GGA	
$a_0$ (Å)	3.64	3.52	3.63	3.61
$E_{[001]}$ (GPa)	67.9	92.4	74.5	67.8
$C'$ (GPa)	25.5	36.4	27.6	25.7
$C_{44}$ (GPa)	78.3	—	82.0	81.7
$\sigma_{E=0}$ (GPa)	24.3	32.4	24.1	—

It may be seen that, in the LDA case, the value of the lattice parameter is substantially lower than the experimental one and computed values of all elastic moduli are significantly higher. On the other hand, the results of the GGA calculations (obtained by both the WIEN97 and the VASP codes) are in a better agreement with the experimental data. Therefore, all our following calculations were performed by means of the VASP code and the GGA.

The computed value of the stress at the inflection point obtained by means of WIEN97 code using the LDA is in a very good agreement with the previous result of 33 GPa of [4] owing to the same approximation being applied. However, the GGA employed together with both the VASP and the WIEN97 codes yields lower values in a better coincidence with the result of 23.7 GPa reported in [6].

The equilibrium lattice constant of the bcc structure was obtained from the computed values of  $E_{\text{tot}}$  as a function of an atomic volume. Our value of  $a_0^{\text{bcc}} = 2.90$  Å is higher than the result of 2.80 Å reported in [23]. On the other hand, it precisely agrees with the result obtained recently by [24] and by [25]. The total energy difference between the bcc and fcc structures is about 36 meV (see figure 2). Slightly higher energy differences of 40 and of 44 meV were reported in [8] and [23], respectively.

The calculated values of the stability conditions related to the elastic constants of the fct lattice are displayed as functions of  $\varepsilon$  in figure 3. Again, the vertical lines represent positions of bcc and fcc structures. In the region of tensile stresses ( $\varepsilon > 0$ ), the stability condition

**Table 2.** Computed values of the stresses  $\sigma$  and the linear extensions  $\varepsilon$  related to the onset of instability in uniaxially deformed Cu along the [001] axis in the region of both the tensile and the compressive loading.

Instability	Tension		Compression	
	$\sigma$ (GPa)	$\varepsilon$ (-)	$\sigma$ (GPa)	$\varepsilon$ (-)
$E_{[001]} = 0$	24.3	0.33	-3.5	-0.09
$C_{11} - C_{12} = 0$	9.4	0.10	—	—
$C_{44} + \sigma/2 = 0$	20.7	0.25	—	—
$C_{66} = 0$	—	—	-0.5	-0.19

$C_{11} - C_{12} > 0$  is broken as the first case at  $\varepsilon = 0.10$ , i.e. well before the inflection point of the  $E_{\text{tot}}(\varepsilon)$  curve (related to the condition  $E_{[001]} = 0$  at  $\varepsilon = 0.33$ ) is reached. The condition  $C_{44} + \sigma/2 > 0$  is also broken before the inflection point ( $\varepsilon = 0.25$ ). The last stability condition  $C_{66} > 0$  remains fulfilled over the whole region of computed tensile strains.

On the other hand, the condition related to the inflection point ( $E_{[001]} > 0$ ) is broken as a first case in the region of compressive strains (at  $\varepsilon = -0.09$ ). Let us note that  $E_{[001]} > 0$  is fulfilled for  $\varepsilon < -0.23$  again; however, the fourth condition  $C_{66} > 0$  is broken for  $\varepsilon < -0.20$ . Therefore, for bcc Cu, two stability conditions are violated.

The fct structure at  $\varepsilon = -0.25$  (corresponding to the shallow minimum in figure 2) exhibits a positive Young modulus in agreement with the calculations for the epitaxial Bain path reported by [8] that yield a shallow minimum for bct structure with  $c/a = 0.927$  (this value of  $c/a$  corresponds to setting  $c/a = 1$  for the bcc structure). However, it is unstable since the condition  $C_{66} > 0$  is violated.

The computed values of stresses and linear extensions corresponding to the failures of the tested stability conditions are shown in table 2. The lowest tensile stress of 9.4 GPa related to breaking the  $C_{11} - C_{12} > 0$  condition in the region of tensile loading is considered to be the theoretical strength of copper crystal under uniaxial tensile loading in the [001] direction. This value corresponds well to the result of 9.8 GPa computed by [6] using the embedded-atom method. The corresponding linear extension  $\varepsilon = 0.10$  is somewhat smaller than their value of 0.13. The stress corresponding to the point of breaking the first stability condition under compression is about 3.5 GPa and the related linear extension is  $-0.09$ .

Where do we search for the source of the discrepancy between the calculated and measured ideal tensile strengths of copper when we suppose that our calculations are correct? First, some defects in whiskers or imperfections of loading devices cannot be excluded [22]. The experiments were performed about 30 years ago; it would be nice to repeat them with the powerful technology available today. A thorough interpretation of nanoindentation experiments could also shed light on this problem. Of course, it is possible that, before violating the first stability condition, some phonon instability may appear in the tetragonally strained crystal. Indeed, recent studies on elastic [26] and phonon instabilities [27] of aluminium confirm the suggestion that this may happen in fcc metals. Therefore, the phonon instabilities will be the subject of future considerations.

#### 4. Conclusions

In the present paper we investigated the mechanical stability of fcc copper under uniaxial loading in the [001] direction. In the region of compressive deformations, the stability condition  $E_{[001]} > 0$  is broken as the first case at the linear extension of  $\varepsilon = -0.09$ . For the bcc structure



obtained at  $\varepsilon = -0.205$ , two stability conditions are already violated. In the region of tensile deformations, we have found the first occurrence of instability at the linear extension of 0.10 related to vanishing of the tetragonal shear modulus. The corresponding stress of 9.4 GPa is therefore considered to be the theoretical strength under uniaxial tension. This value is less than a half of the computed value of  $\sigma_{E=0}$  corresponding to the inflection point of the  $E(\varepsilon)$  curve, but it is still substantially higher than the experimental result of 1.5 GPa [5]. As the defects in whiskers or imperfections of loading device cannot be excluded, we suggest repeating those experiments.

### Acknowledgments

This research was supported by the Grant Agency of the Czech Republic (Project No 202/03/1351), by the Grant Agency of the Academy of Sciences of the Czech Republic (Project No IAA1041302), by the Ministry of Education of the Czech Republic (Project No MSM 262100002), and by the Research Project Z2041904 of the Academy of Sciences of the Czech Republic.

### References

- [1] Pokluda J and Šandera P 1991 *Phys. Status Solidi b* **167** 543
- [2] Van Vliet K J, Li J, Zhu T, Yip S and Suresh S 2003 *Phys. Rev. B* **67** 104105
- [3] Milstein F and Farber B 1980 *Phil. Mag.* **A 42** 19
- [4] Šob M, Wang L G and Vitek V 1998 *Kovové Materiály (Metallic Materials)* **36** 145
- [5] Macmillan M H 1981 *Atomistics of Fracture* ed R M Latanision and J R Pickens (New York: Plenum) p 95
- [6] Milstein F and Chantasiriwan S 1998 *Phys. Rev. B* **58** 6006
- [7] Qiu S L and Marcus P M 1999 *Phys. Rev. B* **60** 14533
- [8] Jona F and Marcus P M 2001 *Phys. Rev. B* **63** 094113
- [9] Wang J, Li J and Yip S 1995 *Phys. Rev. B* **52** 12627
- [10] Morris J W Jr and Krenn C R 2000 *Phil. Mag.* **A 80** 2827
- [11] Morris J W Jr, Krenn C R, Roundy D and Cohen M L 2000 *Phase Transformations and Evolution of Materials* ed P E A Turchi and A Gonis (Warrendale, PA: Minerals, Metals and Materials Society) p 187
- [12] Mehl M J, Osburn J E, Papaconstantopoulos D A and Klein B M 1990 *Phys. Rev. B* **41** 10311
- [13] Murnaghan F D 1951 *Finite Deformation of an Elastic Solid* (New York: Wiley)
- [14] Kresse G and Furthmüller J 1996 *Phys. Rev. B* **54** 11169
- [15] Vanderbilt D 1990 *Phys. Rev. B* **41** 7892
- [16] Perdew J P and Wang Y 1992 *Phys. Rev. B* **45** 13244
- [17] Blaha P, Schwarz K and Luitz J 2000 *WIEN97 User's Guide* Technical University of Vienna
- [18] von Barth U and Hedin L 1972 *J. Phys. C: Solid State Phys.* **5** 1629
- [19] Černý M, Šob M and Šandera P 2001 *Proc. Int. Conf. JUNIORMAT'01* (Brno: Faculty of Mechanical Engineering Brno University of Technology) p 150
- [20] Kittel C 1976 *Introduction to Solid State Physics* (New York: Wiley)
- [21] Overton W C and Gaffney J 1955 *Phys. Rev.* **98** 969
- [22] Kobayashi H and Hiki I 1973 *Phys. Rev. B* **7** 594
- [23] Wang L G and Šob M 1999 *Phys. Rev. B* **60** 844
- [24] Tang Z, Hasegawa M, Nagai Y and Saito M 2002 *Phys. Rev. B* **65** 195108
- [25] Zhou Y, Lai W and Wang J 1993 *Phys. Rev. B* **49** 4463
- [26] Li W and Wang T 1998 *J. Phys.: Condens. Matter* **10** 9889
- [27] Clatterbuck D M, Krenn C R, Cohen M L and Morris J W Jr 2003 *Phys. Rev. Lett.* **91** 135501